Received: 22 April 2019 | Revised: 8 May 2019 | Accepted: 20 May 2019

DOI: 10.1002/ese3.377

Energy Science & Engineering Open Access

RESEARCH ARTICLE

Numerical simulation of boreholes for gas extraction and effective range of gas extraction in soft coal seams

Pan Wei[1,2] | **Changwen Huang**[3] | **Xuelong Li**[1,2] | **Shoujian Peng**[1,2] | **Yanan Lu**[4]

[1]State Key Laboratory of Coal Mine Disaster Dynamics and Control, Chongqing University, Chongqing, China

[2]College of Resources and Environmental Science, Chongqing University, Chongqing, China

[3]Chongqing Energy Technology Investment Group Company Limited, Chongqing, China

[4]College of Safety Science and Engineering, Xi'an University of Science and Technology, Xi'an, China

Correspondence
Shoujian Peng, State Key Laboratory of Coal Mine Disaster Dynamics and Control, Chongqing University, Chongqing 400044, China.
Email: sjpeng@cqu.edu.cn

Funding information
This work was supported by National Key R & D Program of China (2018YFC0808303), the Basic and Frontier Research Projects of Chongqing (cstc2016jcyjA0117, cstc2018jcyjAX0626), and the Fundamental Research Funds for the Central Universities (2017CDJQJ248825).

Abstract

Gas disasters are a major factor influencing safe production in mines: Gas extraction can reduce the gas content in coal seams, providing a guarantee of safer production. The parameters for gas extraction are the primary factors influencing the effectiveness thereof. Aiming at the creep properties of soft coal, a fluid-solid coupling mathematical model considering creep properties of coal was established based on dynamic evolution equation for permeability considering the effects of matrix shrinkage and effective stress. Additionally, by utilizing COMSOL Multiphysics software, the gas extractions from a single borehole and multiple boreholes were calculated. Moreover, the parameters for gas extraction were optimized and applied and tested in field conditions. The result showed the reduction in gas pressure around the boreholes was larger than that from a single borehole when conducting gas extraction from multiple boreholes. The borehole spacing when extracting gas in coal seams by drilling multiple boreholes should be more than twice that of the effective drainage radius. The optimal borehole spacing ranged from 3.2 to 4.2 m for gas extraction lasting 180 d. Numerical simulation was carried out to ascertain the distribution of stress on coal around a roadway. The result revealed that the damage radius of the roadway was 11.8 m, and a reasonable hole-sealing depth was 12 m. On condition that the borehole spacing during gas extraction from multiple boreholes was 4 m, the reasonable pre-extraction time was 180 days taking the gas pressure being reduced to <0.74 MPa as a critical point. Furthermore, the gas content, the amount of extracted gas, etc, in a working face after the parameters for gas extraction were optimized were measured. The result suggested that the effect of gas extraction after optimizing parameters conformed to industry standards.

KEYWORDS

fluid-solid coupling, gas extraction, numerical simulation, parameter optimization, soft coal

1 | INTRODUCTION

According to statistics, China coal mines were subjected to 354 gas accidents during 2007-2017, causing 2655 deaths (Figure 1). The statistical result indicates that the death toll in China's gas accidents during 2007-2017 accounted for more than 40% of the total death toll due to production accidents in coal mines. The number of gas accidents during

2007-2017 accounted for about 45% of the total number of accidents in coal mines.[1] Gas in coal mines is also a green energy source, showing multiple advantages including efficiency and low-pollutant emitting.[2-4] China is rich in gas reserves, ranking second in the world; however, in the process of coal mining, the vast majority of gas cannot be effectively utilized.[5] Moreover, with the constant increase in mining depth, mining conditions become more complex and the hidden dangers during coal mining are significant. In particular, with the increase in mining depth, coal is often softer and the initial gas pressure on coal seams is higher. Thus, the amount of gas emitted from a working face increases so that it is difficult to guarantee safe production[6,7]; therefore, investigating gas control in mines, especially exploring gas extraction from coal seams after coal is softened and undergoes creep deformation caused by increased mining depth, plays a crucial role in guaranteeing the safe and efficient production of mines.

At present, the methods for gas extraction from mines in China mainly include ground and underground gas extraction; however, underground gas extraction is mainly applied at present. Furthermore, according to the source of gas emission, underground gas extraction is divided into gas extraction seam undermining, adjacent seam, goaf, and surrounding rocks.[8] In the majority of China's coal mines, gas is emitted from coal seams undermining, and therefore, gas pre-extraction in coal seams undermining is the primary method for reducing the gas content in coal seams and decreasing the amount of gas emitted from a working face.[5]

Due to the complexity of the conditions of mining coal seams and the occurrence of gas, it is necessary to determine reasonable parameters for gas extraction.[9] Parameters for gas extraction mainly include borehole spacing, hole-sealing depth, and gas pre-extraction time. In the preliminary design stage of gas extraction engineering operations, the parameters for gas extraction are generally determined according to experience-based judgment of engineers, showing a high degree of subjectivity.[10] The reason is that different engineers operate to diverse design standards, and therefore, the resulting parameters for gas extraction are not scientific and show significant discrepancies, which are hard to apply in actual mine conditions. For example, there is no uniform standard in terms of hole-sealing depth. The soft and hard coal as well as other factors are not differentiated, which likely leads to a poor sealing effect around boreholes and conditions unfavorable to gas extraction; an excessive pre-extraction time can present problems to mining and tunneling planning in a coal mine, and impairs efficient production. Too short a pre-extraction time may trigger insufficient gas extraction and thus poses hidden dangers. Additionally, with increasing mining depth, coal strengths also gradually decrease. After long-term gas extraction, hole shrinkage, hole collapse, etc., are likely to occur, and thus, the channel for extracting gas is blocked which reduces the gas extraction rate. Therefore, it is necessary to consider the creep properties of gas-bearing coal when determining the parameters governing gas extraction.

The borehole spacing, parameters of borehole arrangement, the hole-sealing depth, hole-sealing materials, and pre-extraction time during the mining of coal seams are considered as the most important parameters for gas pre-extraction in coal seams undermining conditions.[5,11] The borehole spacing and the borehole layout during gas pre-extraction are both related to the effective radius of gas extraction in a borehole. At present, the methods for measuring effective radius of gas extraction involve field measurement and numerical simulation.[10,12] Field measurement mainly includes pressure reduction methods, flow methods, and tracer gas method (SF_6).[13,14] For numerical simulation, different numerical models are established based on various theoretical bases including stress-strain theory as applied to boreholes in coal, theory of gas seepage in coal, and fluid-solid coupling theory.[15] The calculation is carried out by applying numerical simulation software to determine the effective radius of gas extraction.

Scholars in the former Soviet Union first explored the law of gas seepage in coal by employing Darcy's law. Afterward, on this basis, researchers proposed diverse theories including linear gas diffusion theory, seepage-diffusion theory, nonlinear gas flow, gas flow under the effect of a geophysical field, and gas leakage theory in multiple coal seams. These theories provide a basis for gas extraction technologies. Based on the adsorption mechanism, numerous scholars have established different models such as the Langmuir model,[16,17] Brunauer-Emmett-Teller (BET) model,[18] Polanyi adsorption potential,[19-22] Langmuir-Freundlich adsorption model,[23,24] micropore filling theory,[25,26] and Freundlich Equation.[27] Coal is a typical porous medium. When exploring gas adsorption and desorption

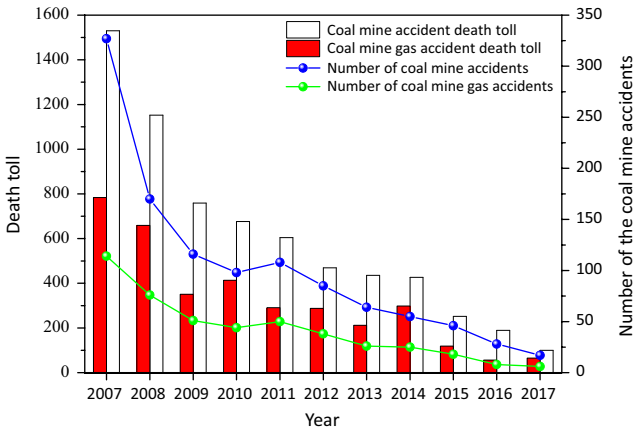

FIGURE 1 Statistics on coal mine accidents from 2010 to 2017. Note: The above data are from the accident investigation system of the Web site of State Administration of Work Safety (SAWS)

behaviors in coal, numerous scholars found that collisions after gas adsorption and desorption in coal influence the flow channel of gas, thus causing changes in the permeability and porosity of coal. The changes in permeability and porosity play an important role in mining coalbed methane (CBM). At present, the permeability of coal seams is investigated mainly through permeability model with a single borehole for elastic deformation, permeability model with dual boreholes considering elastic deformation of coal blocks, etc. The representative permeability models with a single borehole considering elastic deformation[28,29] include Seidle-Huitt,[30-32] Palmer-Mansoori,[33,34] Shi-Durucan,[35,36] Cui-Bustin,[37,38] and Robertson-Christiansen models.[39-41] These models only explore the influence of pore pressure on permeability and porosity on the premise that the external stress remains constant.[42]

When investigating gas extraction through borehole drilling, various aspects (including mechanical properties, seepage characteristics of gas, and solid-gas coupling in coal around the boreholes) need to be taken into account. Therefore, according to the creep and mechanical properties of coal, the governing equation for deformation of coal around boreholes was established. Moreover, based on the dynamic evolution equation for permeability considering the effects of matrix shrinkage and effective stress, a fluid-solid coupling mathematical model considering the creep characteristics of coal was constructed. The gas extraction process was calculated by applying COMSOL Multiphysics numerical simulation software. Furthermore, based on the result obtained through numerical simulation, the parameters for gas extraction were optimized and then verified according to gas extraction yield measured in situ. Benefit analysis was also conducted to assess the effects of parameter optimization.

2 | MATERIALS AND METHODS

2.1 | Properties of coal samples

The mine for the test is located in Weinan, Shaanxi Province, China, and it is a new mine in the western region of the mining area (Figure 2). The working face has a mining height of 4 m, with lengths at the strike and trend of 2000 and 150 m, respectively. The permo-carboniferous 5# coal seam was primarily mined, and the basic parameters relating to the gas therein are listed in Table 1.

As shown in Table 1, the 5# coal seam is classified as a soft coal, showing a large initial velocity of gas diffusion. A large initial velocity of gas diffusion in coal seams reflects the fact that the velocity of gas emission from coal seams is large when soft coal is first exposed.

2.2 | COMSOL Multiphysics simulation calculation process

By using the PDE (partial differential equation) module in COMSOL Multiphysics, numerical simulation of gas extraction operations in coal seams under different conditions and parameters is undertaken (Figure 3).

3 | THEORETICAL MODEL

3.1 | Basic assumptions

Gas migration is a complex process influenced by multiple factors. During numerical simulation, only the main factors influencing gas seepage are taken into account due to the limitations of the simulation. Therefore, it is necessary to

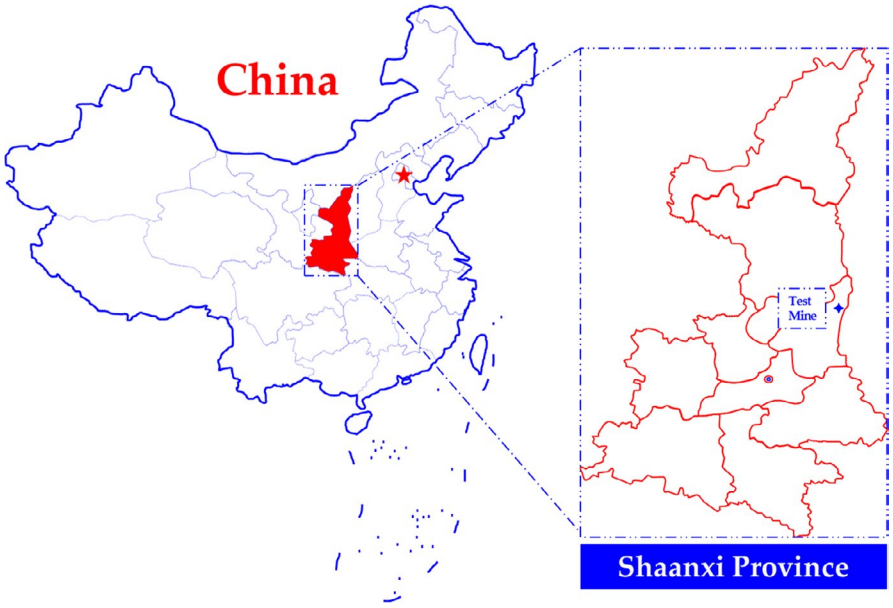

FIGURE 2 Geographic location of the test mine

TABLE 1 Coal sample basic parameters

Sample	Protodyakonov coefficient (f)	Initial speed of methane diffusion (Δp) (mL/s)	Porosity (%)	Industrial analysis		
				A_{ad} (%)	M_{ad} (%)	V_{daf} (%)
HY	0.93	22.27	11.19	33.28	0.54	18.35

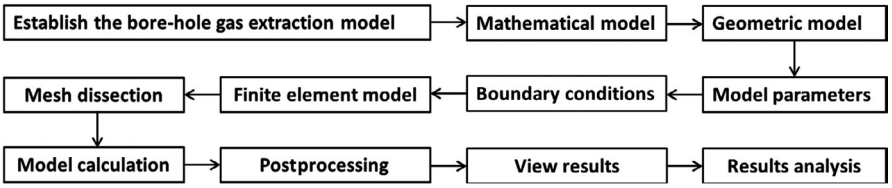

FIGURE 3 COMSOL Multiphysics calculation process

eliminate the restriction of some unimportant factors on simulation so as to simplify the process of gas seepage. Aiming at gas migration, the following assumptions are made.[10]

1. Gas-bearing coal seams are isotropic, homogeneous, porous media;
2. Gas in coal seams is desorbed instantaneously, and gas adsorption in coal seams satisfies the Langmuir equation;
3. Gas seepage in coal seams conforms to Darcy's law;
4. Gas in coal seams is an ideal gas;
5. The surrounding rocks in the roof and floor of coal seams are gas-tight, and there is no gas therein.

3.2 | Governing equations

3.2.1 | Governing equation for flow field of gas in boreholes

Gas migration in coal seams is a complex process influenced by multiple factors while conforming to the law of conservation of mass. Accordingly, the equation of continuity for gas seepage[43] is shown in Equation (1).

$$\frac{\partial M}{\partial t}+\nabla\cdot(\rho\cdot v)=0 \tag{1}$$

where, M, ρ, v, and t refer to the mass (m^3/kg) of gas in unit volume of coal, gas density (kg/m^3) of coal seams, seepage velocity (m/s) of gas, and time (seconds), respectively.

According to Equation (2) for gas content,

$$\frac{\partial M}{\partial t}=\frac{\partial M_x}{\partial t}+\frac{\partial M_y}{\partial t}=\frac{\beta abcP_n}{(1+bP)^2}\frac{\partial P}{\partial t}+\beta\left(\frac{P(1-\varphi_0)}{(1+\varepsilon_v)^2}\frac{\partial \varepsilon_v}{\partial t}+\frac{\varphi_0+\varepsilon_v}{1+\varepsilon_v}\frac{\partial P}{\partial t}\right) \tag{2}$$

where M_x, M_y, a, and b denote the content (m^3/kg) of adsorbed gas, the content (m^3/kg) of free gas, adsorption limit (m^3/t) of coal (an adsorption constant), and an adsorption constant (MP^{-1}), respectively. Moreover, ρ_n, ρ_s, and c represent the gas density (kg/m^3) at standard atmospheric pressure, the density (kg/m^3) of coal, and corrected parameter $c=\rho_s\left(\frac{1}{1+0.147e^{0.022V_{ad}}}e^{n(T_S-T)}\right)\frac{100-M_{ad}-A_{ad}}{100}$ (kg/m^3, $n=\frac{0.02}{0.993+0.07P}$) of coal, respectively. Additionally, T_s, T, M_{ad}, V_{ad}, and A_{ad} denote the temperature (°C) of the laboratory during adsorption testing, the temperature (°C) of underground coal, the water content (%) of the coal, the amount (%) of volatile matter in coal, and the ash content (%) in coal, respectively.

According to Darcy's law,[44] the seepage velocity of gas in coal seams can be obtained.

$$v=-\frac{k}{\mu}\cdot\nabla P \tag{3}$$

where, P, k, and μ denote gas pressure (MPa), the permeability (m^2) of coal seams, and the dynamic viscosity coefficient (Pa·s) of gas, respectively.

By substituting Equations (2) and (3) into Equation (1), the governing equation for gas flow in a fluid-solid coupling model for coal around the boreholes is given by Equation (4):

$$\frac{2P(1-\varphi_0)}{(1+\varepsilon_v)^2}\frac{\partial \varepsilon_v}{\partial t}+\frac{\varphi_0+\varepsilon_v}{P(1+\varepsilon_v)}\frac{\partial P^2}{\partial t}+\frac{abcP_n}{(1+bP)^2}\frac{\partial P^2}{\partial t}=\nabla\cdot\left(\frac{K}{\mu}\cdot\nabla P^2\right) \tag{4}$$

3.2.2 | Governing equation for the deformation of coal around the boreholes

The mechanical model for coal around the boreholes[45] is shown in Figure 4. According to the law governing the deformation of coal around the boreholes, a certain zone within the coal is partitioned into an elastic zone (e), a plastic zone (p), and a broken zone (b) from the outside to the inside. After

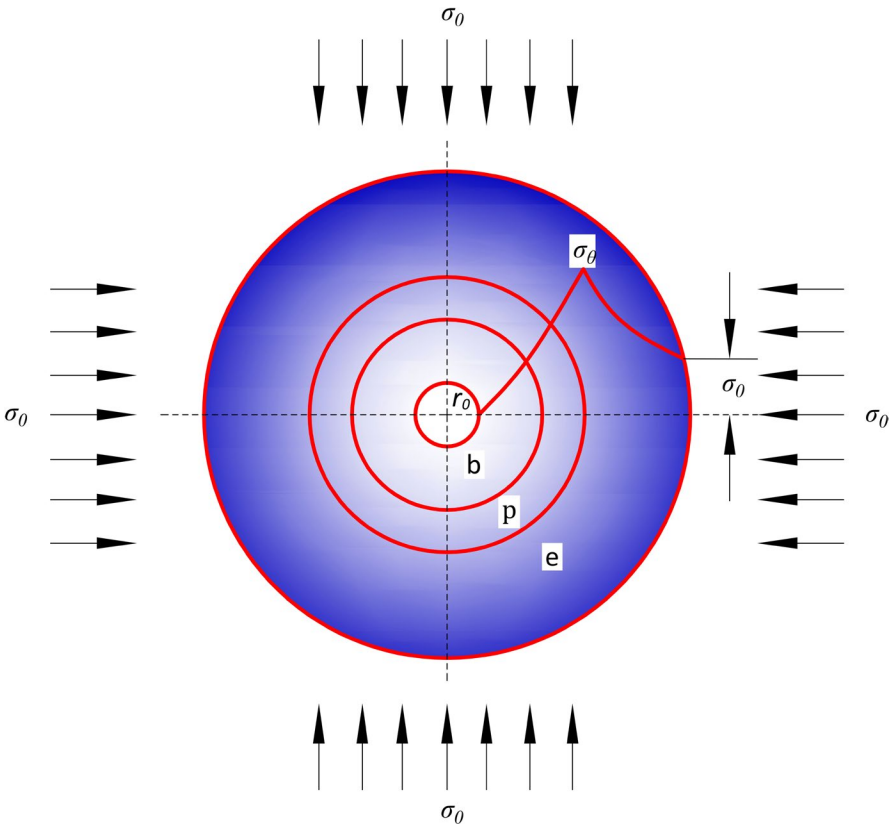

FIGURE 4 Mechanical model for coal around the boreholes. Note: σ_0, σ_θ, and r_0 refer to initial geostress, tangential stress, and initial hole diameter, respectively

boreholes for gas extraction are formed, three damaged zones are formed around the boreholes.

Plane strain analysis is conducted to assess the deformation, which satisfies equilibrium Equation (5) and geometrical Equation (6):

$$\frac{d\sigma_r}{dr}+\frac{\sigma_r-\sigma_\theta}{r}=0 \tag{5}$$

$$\begin{cases}\varepsilon_r=\dfrac{du}{dr}\\ \varepsilon_\theta=\dfrac{u}{r}\end{cases} \tag{6}$$

where σ_r, σ_θ, ε_r, ε_θ, u, and r represent the radial and tangential stresses (MPa) on the coal, radial and tangential strains in the coal, radial displacement (mm) of coal around the boreholes, and the distance (m) to the centers of the boreholes, respectively.

According to Equations (5) and (6) and the boundary condition whereby the radial stress on the wall of a borehole is zero, the stress-strain equation of coal around the boreholes can be attained,[46,47] where the displacement (u_0) of the wall of a borehole can be calculated by using Equation (7).

$$u_0=2A(t)\,r_0\left\{\left\{\frac{1}{\eta_1+1}+\frac{1}{\eta_2+1}\left[\left(\frac{R_{b(t)}}{r}\right)^{\eta_2+1}-1\right]\right\}\left(\frac{R_{p(t)}}{R_{b(t)}}\right)^{\eta_1+1}+\frac{\eta_1-1}{2(\eta_1+1)}\right\} \tag{7}$$

where $A(t)$ refers to a function taking time as a dependent variable, $A(t)=\frac{\sigma_0(K_p-1)+\sigma_c}{2(K_p+1)}\left[\frac{1}{G_\infty}\left(1-e^{-\frac{t}{\eta_{ret}}}\right)+\frac{1}{G_0}e^{-\frac{t}{\eta_{ret}}}\right]$; r_0, t, φ, η_1, and η_2 denote the initial diameter of boreholes, time, internal friction angle, dilatancy coefficient of coal in plastic, and viscoelastic softening zones, respectively. Moreover, $R_{b(t)}$ and $R_{p(t)}$ denote the radius of the broken zone and radius ($R_p(t)=NR_b(t)$) of the plastic softening zone, respectively. Additionally, σ_0, σ_c, K_p, G_∞,G_0, and η_{ret} refer to the initial geostress, uniaxial compressive strength of coal, the slope ($K_p=\frac{1+\sin\varphi}{1-\sin\varphi}$) of the yield surface, long-term shear modulus of coal, initial shear modulus of coal, and delay time caused by rheology of soft coal, respectively. Moreover, N, M_c, and σ_c^* represent the ratio ($N=\left[1+\frac{(1+\eta_1)(\sigma_c-\sigma_c^*)}{2A(t)M_c}\right]^{\frac{1}{1+\eta_1}}$) of radius of the plastic softening

$$\left(R_b(t)=\left\{\left\{\left[\sigma_0+\frac{\sigma_c}{K_p-1}+\frac{(K_p+1)M_cA(t)}{(K_p-1)(K_p+\eta_1)}\right]\frac{2}{K_p+1}N^{1-K_p}+\left(\frac{N^{1+\eta_1}}{K_p+\eta_1}-\frac{1}{K_p-1}\right)\frac{2M_cA(t)}{1+\eta_1}-\frac{\sigma_c}{K_p-1}\right\}\frac{K_p-1}{\sigma_c^*}+1\right\}^{\frac{1}{K_p-1}}\right)$$

zone to that of the broken zone, softening modulus, and residual strength of coal, respectively.

The deformation of damaged coal can be considered as the sum of radial and tangential strains in the coal, as shown in Equation (8)[48]:

$$\varepsilon_v = \varepsilon_r + \varepsilon_\theta \tag{8}$$

where ε_v refers to the deformation of coal.

According to the analysis of volumetric strains in broken, plastic, and elastic zones of damaged coal, the mathematical model for volumetric strain in coal around a borehole, considering creep deformation, is expressed as follows:

$$\begin{cases} \varepsilon_v = 0, r \geq R_{p(t)} \\ \varepsilon_v = \dfrac{2A(t)\cdot(1-\eta_1)}{1+\eta_1}\left[\dfrac{R_{p(t)}}{r}\right]^{\eta_1+1} + 2A(t)\dfrac{\eta_1-1}{\eta_1+1}, R_{p(t)} \geq r \geq R_{b(t)} \\ \varepsilon_v = 2A(t)\left\{\dfrac{2}{\eta_1+1} - \dfrac{2}{\eta_2+1} + \dfrac{1-\eta_2}{1+\eta_2}\left(\dfrac{R_{b(t)}}{r}\right)^{\eta_2+1}\right\}\left(\dfrac{R_{p(t)}}{R_{b(t)}}\right)^{\eta_1+1} + 2A(t)\dfrac{1-\eta_1}{1+\eta_1}\left(\dfrac{R_{p(t)}}{R_{b(t)}}\right)^{\eta_1+1} + 4A(t)\dfrac{\eta_1-1}{\eta_1+1}, R_{b(t)} \geq r \geq r_0 \end{cases} \tag{9}$$

3.2.3 | Fluid-solid coupling equation for gas migration during gas extraction

In essence, the gas seepage in coal seams is equivalent to the unsTABLE flow of compressible fluids in anisotropic and heterogeneous porous media. During gas extraction from a coal seam, the initial gas pressure in the coal seam decreases and the gas is constantly changed from an adsorbed state to a free state through desorption to migrate further within the coal seam. In the process, the gas permeability of coal seams changes. The main reasons influencing the change in gas permeability involve matrix shrinkage and effective stress effects. The former refers to the fact that, with the reduction of gas pressure in a coal seam, the adsorbed gas was desorbed from matrix and pores in the coal to result in further shrinkage of the coal matrix and changes to the physical properties of coal reservoirs. The effective stress effect means that the effective stress increases on the coal seam, and therefore, the coal mass is compacted as the gas pressure in coal reservoir decreases, thus decreasing the porosity of the coal.

According to the Kozeny-Carman[49] and Langmuir equations,[16,17] based on the governing equation for flow field of gas in boreholes and that for the deformation of coal around a borehole, the fluid-solid coupling model for coal around the boreholes is attained, as shown in Equation (10): This is calculated by applying the PDE module, and then, the process of gas extraction is simulated by setting different conditions and parameters.

$$\begin{cases} \dfrac{2P(1-\varphi_0)}{(1+\varepsilon_v)^2}\dfrac{\partial\varepsilon_v}{\partial t} + \dfrac{\varphi_0+\varepsilon_v}{P(1+\varepsilon_v)}\dfrac{\partial P^2}{\partial t} + \dfrac{abcP_n}{(1+bP)^2}\dfrac{\partial P^2}{\partial t} = \nabla\cdot\left(\dfrac{k}{\mu}\cdot\nabla P^2\right) \\ k = \dfrac{k_0}{1+\varepsilon_V}\left\{1 + \dfrac{\varepsilon_V}{\varphi_0} - \dfrac{k_Y(P_0-P)(1-\varphi_0)}{\varphi_0} + \dfrac{2a\rho_s RTk_Y}{9V\varphi_0}\left[\ln(1+bP_0) - \ln(1+bP)\right]\right\}^3 \end{cases} \tag{10}$$

where c, μ, P_n, k_0, k_Y, and P_0 refer to the correction coefficient of coal, dynamic viscosity of gas, standard atmospheric pressure, initial permeability, volume compression coefficient, and initial gas pressure, respectively. Moreover, φ_0, P, ρ_s, R, V, and T denote the initial porosity, initial gas pressure on the coal seam, apparent density of coal, universal gas constant, molar volume of gases, and absolute temperature, respectively.

4 | ANALYSIS OF NUMERICAL SIMULATION RESULTS

4.1 | Simulation of effective radius of gas extraction and its analysis

4.1.1 | Geometric model and mesh generation diagram

By considering the actual conditions of field working face and basic assumptions, a two-dimensional (2-d) plane model for gas extraction with the length of 30 m and width of 5 m is established. Moreover, single and multiple boreholes (with a certain spacing) for gas extraction with a diameter of 0.09 m were established in the middle of the model. By utilizing automatic mesh generation, the meshes around the boreholes were refined. The model and mesh generation diagram are shown in Figure 5.

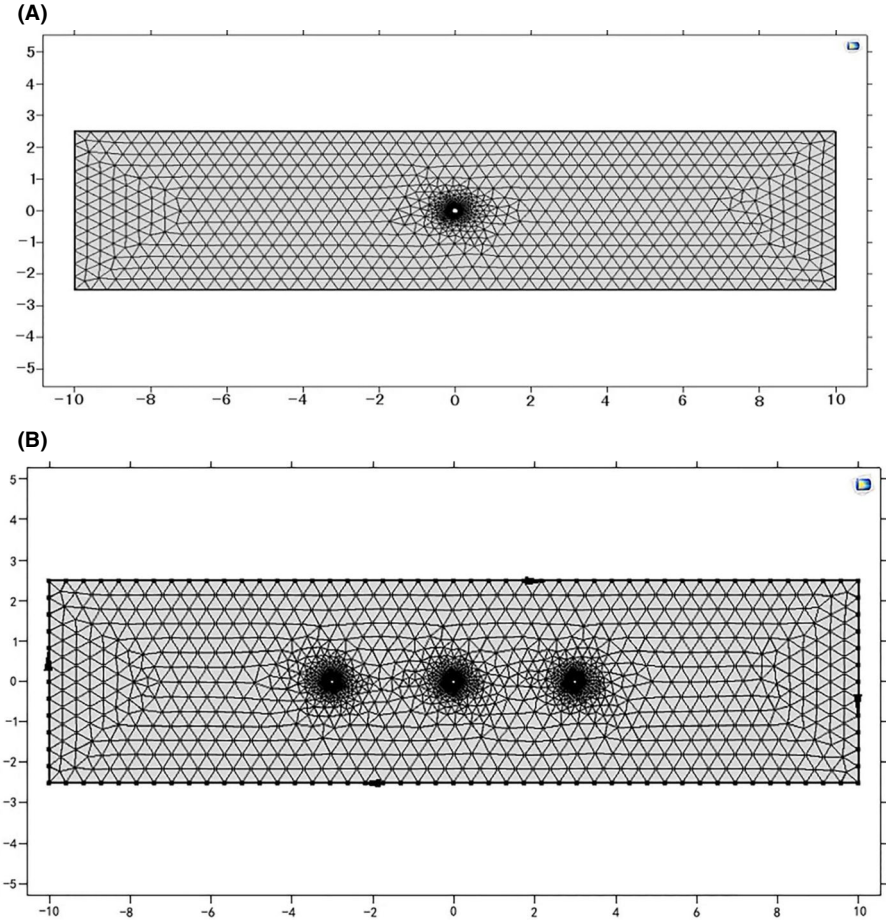

FIGURE 5 The model for effective radius of gas extraction from a borehole and the mesh generation

TABLE 2 Basic physical parameters of the model

Parameters	Value	Unit	Parameters	Unit	Value
Initial porosity,φ_0	0.04		Uniaxial compressive strength,σ_c	8.14	MPa
Dynamic viscosity of gas,μ	1.12×10^{-6}	Pa·s	Residual strength,σ_c^*	0.18	MPa
Adsorption constant,a	22.66	$m^3 \cdot t^{-1}$	Internal friction angle,ϕ	27	°
Adsorption constant,b	1.34	MPa^{-1}	Instantaneous shear modulus,G_0	800	MPa
Density of coal,ρ_s	1.33	$kg \cdot m^{-3}$	Long-term shear modulus,G_∞	400	MPa
Universal gas constant, R	8.314	$J \cdot (mol \cdot K)^{-1}$	Biot coefficient,α	0.3	
Absolute temperature, T	295	K	Protodyakonov coefficient, f	0.93	
Molar volume of gases, V	0.0224	$m^3 \cdot mol^{-1}$			

4.1.2 | Calculation parameters of the model

Boundary conditions: It is supposed that the roof and floor of coal seams belong to air-tight strata. The bottom of the model is a fixed boundary while the top boundary bears a 12.5 MPa overburden pressure. Moreover, the left and right sides are set as free boundaries.

Initial condition: The initial gas pressure of coal seams to be pre-extracted is set to 1.30 MPa, and the negative pressure in boreholes during extraction is 20 kPa.

The other main parameters are displayed in Table 2.

4.1.3 | Analysis of simulation of gas extraction from a single borehole

As shown in Figure 6, upon gas extraction from a single borehole, the gas pressure in coal seams around the borehole constantly decreased and the radius of influence of the borehole for gas extraction constantly expanded. The radius of influence showed a positive correlation with the gas extraction time. The changes in gas pressure around the borehole with time based on the simulation result are shown in Figure 7. The curve has a convex shape, and the gas pressures around

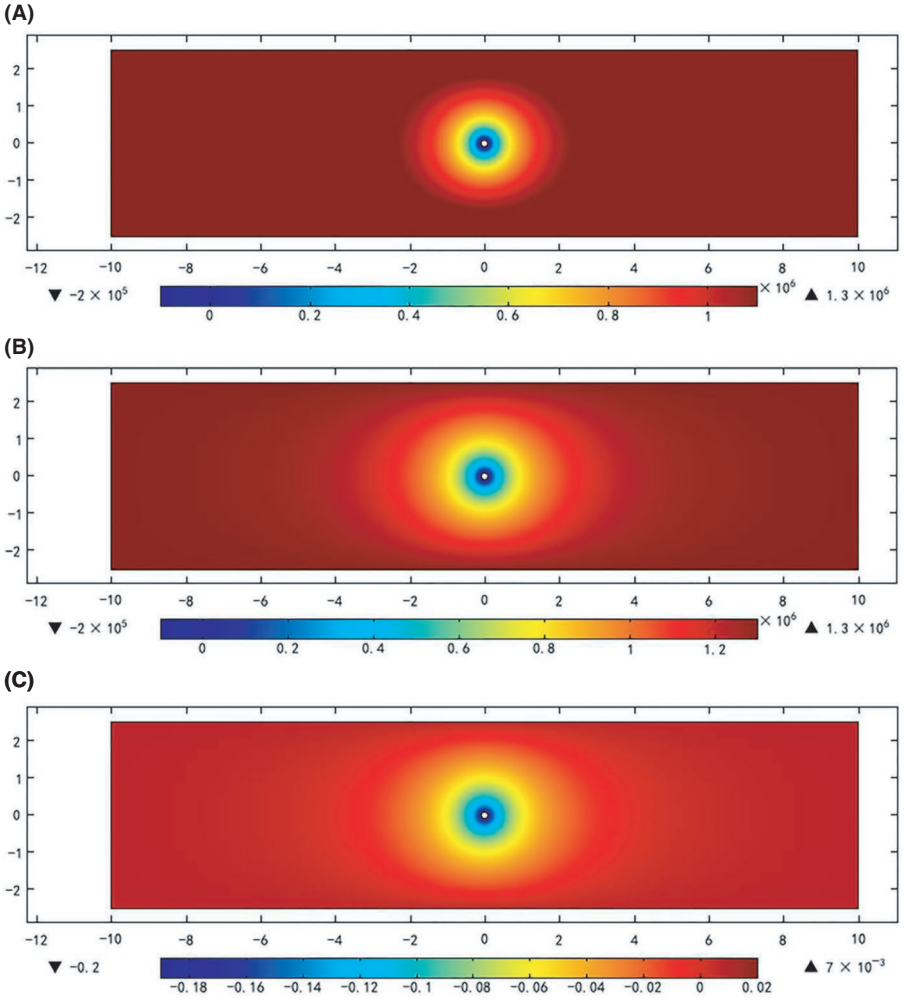

FIGURE 6 Nephogram of gas pressure around the borehole at different extraction times

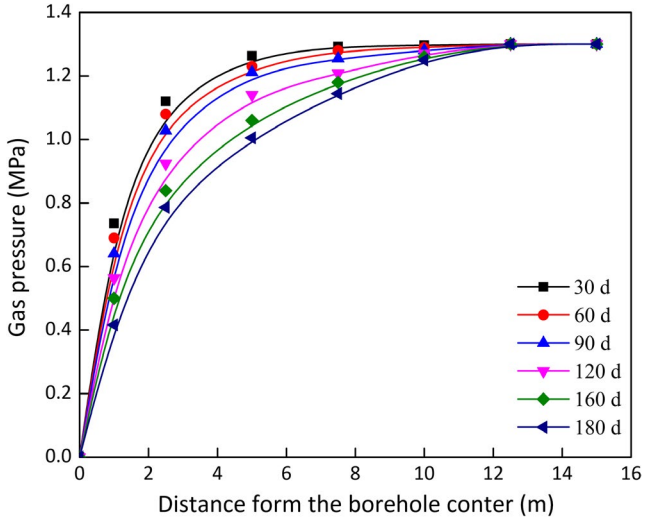

FIGURE 7 Change in gas pressure around a borehole after different extraction times

the borehole at the 30th, 90th, 120th, 160th, and 180th days of gas extraction can be accurately calculated. Furthermore, it can be seen that the radius of influence of the borehole increased with increasing extraction time and gradually stablized.

Based on Figures 6 and 7, it can be seen that the radius of influence of the borehole for gas extraction on the gas pressure in a coal seam was related to the extraction time. The radii of influence on gas pressure at the 30th and 180th day of gas extraction were 0.81 and 1.58 m, respectively. The latter was 1.9 times greater than the former. The radius of influence of the borehole on gas pressure in a coal seam increased with increasing extraction time and gradually stabilized. The reason for this was that, in the early stage of gas extraction, various phenomena (such as a large gradient of gas pressure around the borehole, and collapse and shrinkage of the borehole) were insignificant and the adsorbed gas was more likely to have been desorbed after coal failure. As a result, the seepage velocity of gas was large, leading to a large rate of reduction of gas pressure in the coal seam. In the later stage of gas extraction, the gradient of gas pressure around the borehole decreased and the borehole also collapsed and shrank. Therefore, the rate of reduction in gas pressure in coal seams was low, thus resulting in a reduced gas extraction rate.

During gas extraction from coal seams, the contours showing where the gas pressure after gas extraction declined by 10% and 50% compared with the initial gas pressure were separately considered as the radius of influence and effective radius of gas extraction. Based on the standard and simulated result, the influence radius and effective radius of the borehole for gas extraction at the 30th, 90th, 120th, 150th, and 180th day of gas extraction are as listed in Table 3.

TABLE 3 The radius of influence and effective radius of gas extraction from a single borehole

Gas extraction time/d	Radius of influence *R*/ m	Effective radius *r*/ m
30	2.83	0.81
60	4.07	0.92
90	5.11	1.13
120	6.08	1.30
150	6.91	1.45
180	7.72	1.58

4.1.4 | Analysis of simulated gas extraction from multiple boreholes

During practical gas extraction in mines, multiple adjacent boreholes for gas extraction were installed. In this case, gas migration around the boreholes was influenced by negative pressures in adjacent boreholes. Therefore, it is necessary to consider the superposition effect during gas extraction in mines. In the simulation, by considering the superposition effect, the process of gas extraction under the same extraction time yet at different borehole spacings was simulated to determine the optimal borehole spacing.

The nephogram of gas pressures at borehole spacings of 2.4, 3.2, and 4.0 m at the 180th day of the gas extraction from multiple boreholes is shown in Figure 8. By analyzing Figure 8, it can be seen that, after the same extraction time and for the same number of boreholes, the smaller the borehole spacing, the lower the radius of influence of boreholes for gas extraction, which was unfavorable for gas extraction and vice versa. Therefore, it is feasible to guarantee the safe production and maximize the radius of influence of the boreholes by selecting a reasonable borehole spacing. Compared with the nephogram of gas pressure of coal seams after being

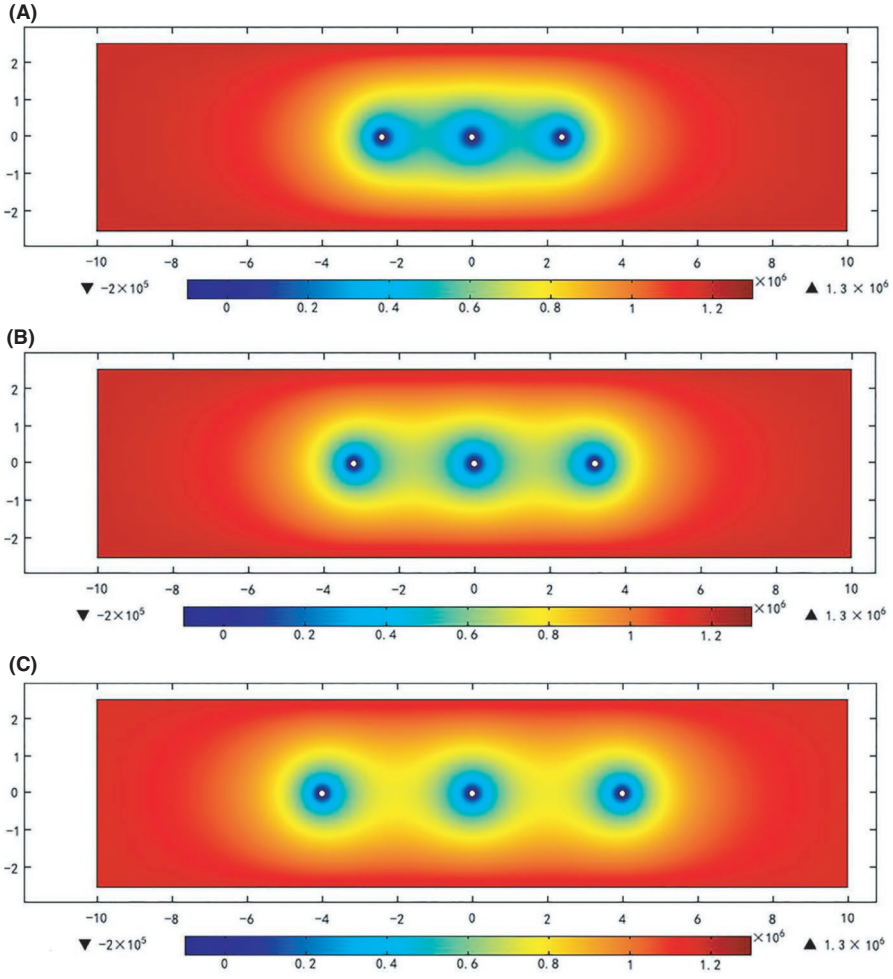

FIGURE 8 Nephogram of gas pressure after 180 d of gas extraction for different borehole spacings

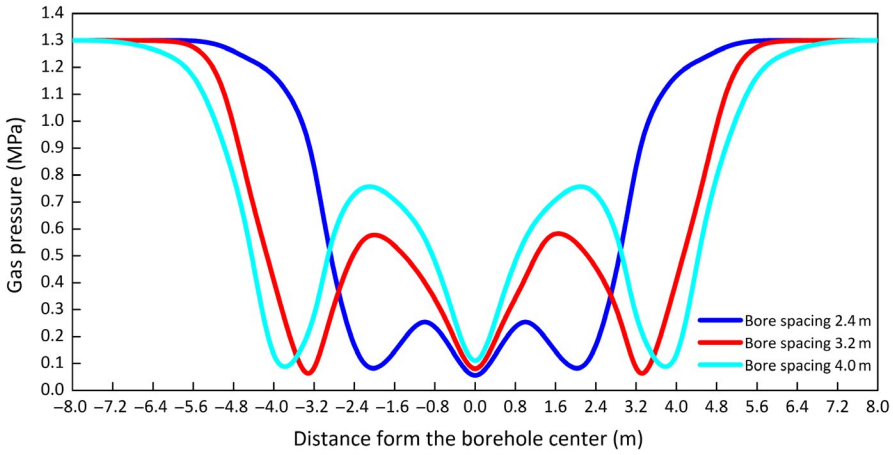

FIGURE 9 Distribution of gas pressure in coal seams at the 180th d of gas extraction from multiple boreholes

subjected to extraction from a single borehole, the radius of influence of boreholes for gas extraction was larger during gas extraction from multiple boreholes due to the superposition of the effects thereof. Additionally, the reduction rate of gas pressure of coal seams was larger. The reason for this was that, during gas extraction from multiple boreholes, the gas in coal seams was subjected to superposition effects from two adjacent boreholes, so that the negative pressure of gas during extraction and the flow channel of gas increased, which was conductive to gas extraction. Therefore, the rate of reduction of gas pressure in the coal seam increased.

According to the nephogram of gas pressure at the 180th day of gas extraction, the broken line graph of gas pressure is drawn, as shown in Figure 9. According to the figure, it can be seen that if the borehole spacing was 2.4 m, the gas pressure between two adjacent boreholes declined by 73%. This indicated that the reasonable borehole spacing can be safely increased. At a borehole spacing of 3.2 m (twice the effective radius), the gas pressure between the two adjacent boreholes decreased by 58%. This implied that the borehole spacing should be more than twice the effective radius. As the borehole spacing was 4.0 m, the gas pressure between the two adjacent boreholes was decreased by 38%. This suggested that the borehole spacing should be <4.0 m. Therefore, analyzing the relationship between the borehole spacing and effective radius of gas extraction is important.

The range of influence of boreholes for gas extraction on gas pressure can be divided into strong and weak areas of influence. The scope, where gas pressure after gas extraction declined at least by 50% compared with the initial gas pressure, is the strong influence area, that is, the area within the effective radius of gas extraction. That where the gas pressure after gas extraction fell below 50% of the initial gas pressure is classified as the weak influence area. The boreholes for gas extraction show diverse influences on gas migration within the strong and weak areas of influence. Gas migration within the strong influence areas is mainly influenced by negative pressure in the boreholes during extraction while that within the weak influence area is subjected to superposition effects of the negative pressures in the borehole and adjacent boreholes during extraction. Moreover, when the gas migration within a weak influence area is influenced by the extraction from the boreholes and its neighbors, the effect of gas extraction in the weak influence area can be regarded as that of a strong influence area. By simulating the process of gas extraction under different borehole spacings and analyzing the effects of gas extraction in other working faces of the mine, it can be found that the area was 0.35 times that of the area within the radius of influence of gas extraction. On this basis, the relationship between the borehole spacing and the effective radius and radius of influence of gas extraction is as follows:

$$2r \le L \le r + 0.35R \tag{11}$$

where r, L, and R represent the effective radius (m) of gas extraction from a single borehole, borehole spacing (m), and the radius (m) of influence of gas extraction from a single borehole, respectively.

According to Equation (11) and the simulation result, it can be obtained that the optimal borehole spacing at the 180th day of gas extraction was between 3.2 and 4.2 m.

4.2 | Determination of reasonable hole-sealing depth

Once the construction of an underground roadway starts, fractures in the coal seams become more developed as mining progresses. Hence, an optimal hole-sealing depth is important for gas extraction. It is stipulated in China's *Provision and Control on Coal and Gas Outbursts* that the hole-sealing depth of boreholes should not be <8 m; however, the hole-sealing depth is related to various factors including initial geostress on the coal seam, the coal strength, and supporting stress. Due to the differences in geological factors and mining conditions, the hole-sealing depth varies widely across different mines.

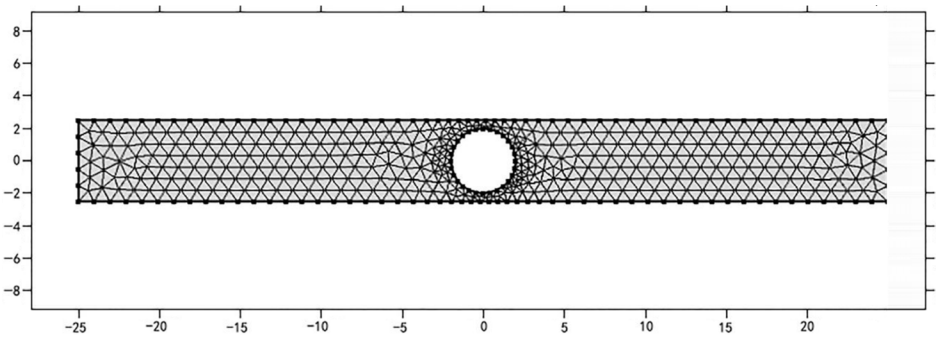

FIGURE 10 Geometric model and mesh generation diagram

4.2.1 | Geometric model and mesh generation diagram

It is supposed that the roadway has as a circular section. On this basis, the stress distribution around the roadway is simulated and analyzed to determine the radius of the broken zone of the roadway, thus calculating the optimal hole-sealing depth. A 2-days geometric model of 40 m in length and 5 m in height is established, and a circle with a diameter of 4 m is established in the middle of the model to simulate the roadway section. By utilizing automatic mesh generation, the mesh around the section of the roadway was refined. The geometric model and mesh generation diagram are shown in Figure 10.

4.2.2 | Model parameters

Boundary condition: Due to being influenced by overburden pressure, the top of the model is set as a stress boundary while the bottom of the model is designed as a fixed boundary. Moreover, the left and right-hand sides of the model are considered as free boundaries and the supporting stress on the roadway is calculated thus $P_0 = \left(\sigma_r^b\right)_{r=r_0}$.

Initial condition: The initial geostress and anchoring force are 12.5 and 0.25 MPa, respectively.

4.2.3 | Analysis of the results related to the hole-sealing depth

The distributions of radial and tangential stresses on coal around the roadway are shown in Figure 11: Due to the tunneling of the roadway, the initial stress state in the coal seams is perturbed, and therefore, stresses are redistributed. In this case, different broken areas are successively formed at the two sides of the roadway. Based on the distribution of tangential stress around the periphery of the roadway, it can be inferred that the tangential stress on the coal in the vicinity of the roadway rises stably with increasing distance from the roadway. Furthermore, the stress rapidly decreases after

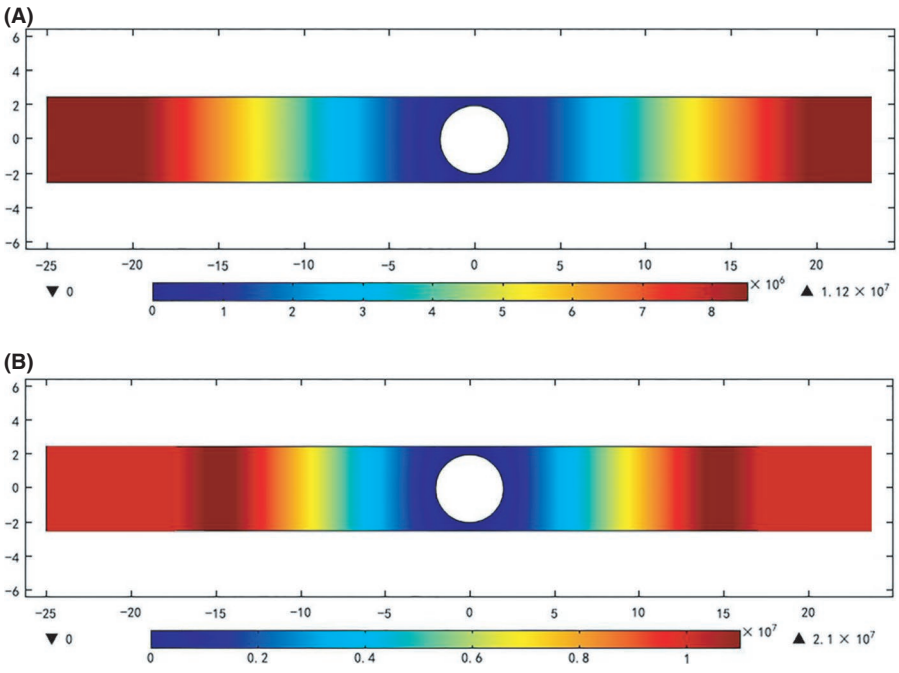

FIGURE 11 Nephogram of distributions of radial and tangential stresses on the periphery of the roadway

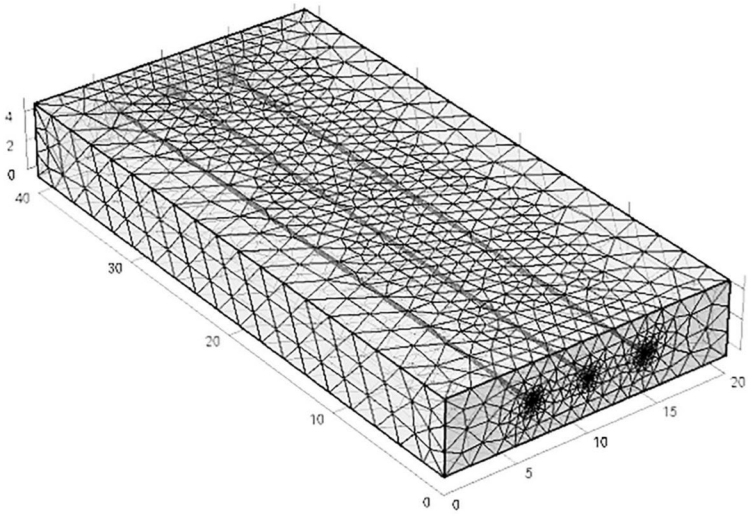

FIGURE 12 Geometric model and mesh generation diagram

reaching its peak value, which means that the zone of peak stress can be regarded as the boundary of the broken zone.

The shallow sealing depth of boreholes corresponds to the stress concentration zone of the roadway. Under negative pressure, a loop circulatory system is formed between the boreholes with fractures and the external space. Under this circumstance, the air in the roadway flows into the boreholes for gas extraction to reduce the concentration of gas extracted. Moreover, the negative pressure of gas in a coal seam declines so as to shorten the time for gas extraction and even prevent its extraction.

It is determined that the area which is the most influenced by the hole-sealing depth is the broken zone, with its radius of 11.8 m. When the hole-sealing depth exceeds the radius of the broken zone, the flow channel for air flows under negative pressure in boreholes during extraction, and many pores and fractures in this zone are blocked. As a result, the influence of air leakage from boreholes on gas extraction is insignificant, which is conducive to gas extraction in coal seams. Based on the radius of broken zone of the roadway obtained through simulation, the best hole-sealing depth was deemed to be 12 m.

4.3 | Determination of reasonable pre-extraction time

Pre-extraction time is one of the important parameters affecting gas extraction. The longer the pre-extraction time, the more favorable it is to reducing the gas pressure in a coal seam: However, an excessive pre-extraction time can pose a challenge to safe mining and tunneling, thus influencing productivity. Too short a pre-extraction time causes less reduction in gas pressure, failing to guarantee safe production; therefore, determining an optimal pre-extraction time plays a crucial role in improving the yield and guaranteeing safe production. The reasonable pre-extraction time of coal seams is a certain extraction time set in order to realize the expected effect of gas extraction on the premise that parameters for gas extraction all conform to actual mining conditions. The index for reasonable pre-extraction time is determined as the extraction time required for the gas pressure in a coal seam to fall to <0.74 MPa.

The simulation scheme for calculating the reasonable pre-extraction time is as follows: Based on the borehole spacing for gas extraction obtained in Section 4.24.2, the gas pressures of coal seams at the 30th, 90th, 180th, and 210th day of gas extraction from multiple boreholes are simulated. The extraction time, during which the maximum gas pressure around the boreholes is less than 0.74 MPa, is considered as the optimal pre-extraction time.

4.3.1 | Geometric model and mesh generation diagram

According to conditions at the working face of the mine, a 3-d model (length × width×height: 20 × 40 × 4 m) is established. Moreover, three boreholes with a diameter of 0.09 m were established in the middle of the model at a spacing of 4 m. By using automatic mesh generation, the mesh in the vicinity of each borehole was refined. The geometric model and mesh generation diagram are displayed in Figure 12.

4.3.2 | Model calculation parameters

Boundary condition: The top and bottom of the model are set as fixed boundaries while the left and right-hand sides are free boundaries.

Initial condition: The initial gas pressure and negative pressure during gas extraction are set to 1.3 MPa and 20 kPa, and the initial gas permeability coefficient of coal is 1.533 $m^2 \cdot MPa^{-2} \cdot d^{-1}$.

4.3.3 | Simulation of pre-extraction time and its analysis

The gas pressures at the 30th, 90th, 180th, and 210th day of gas extraction are shown in Figure 13: The maximum

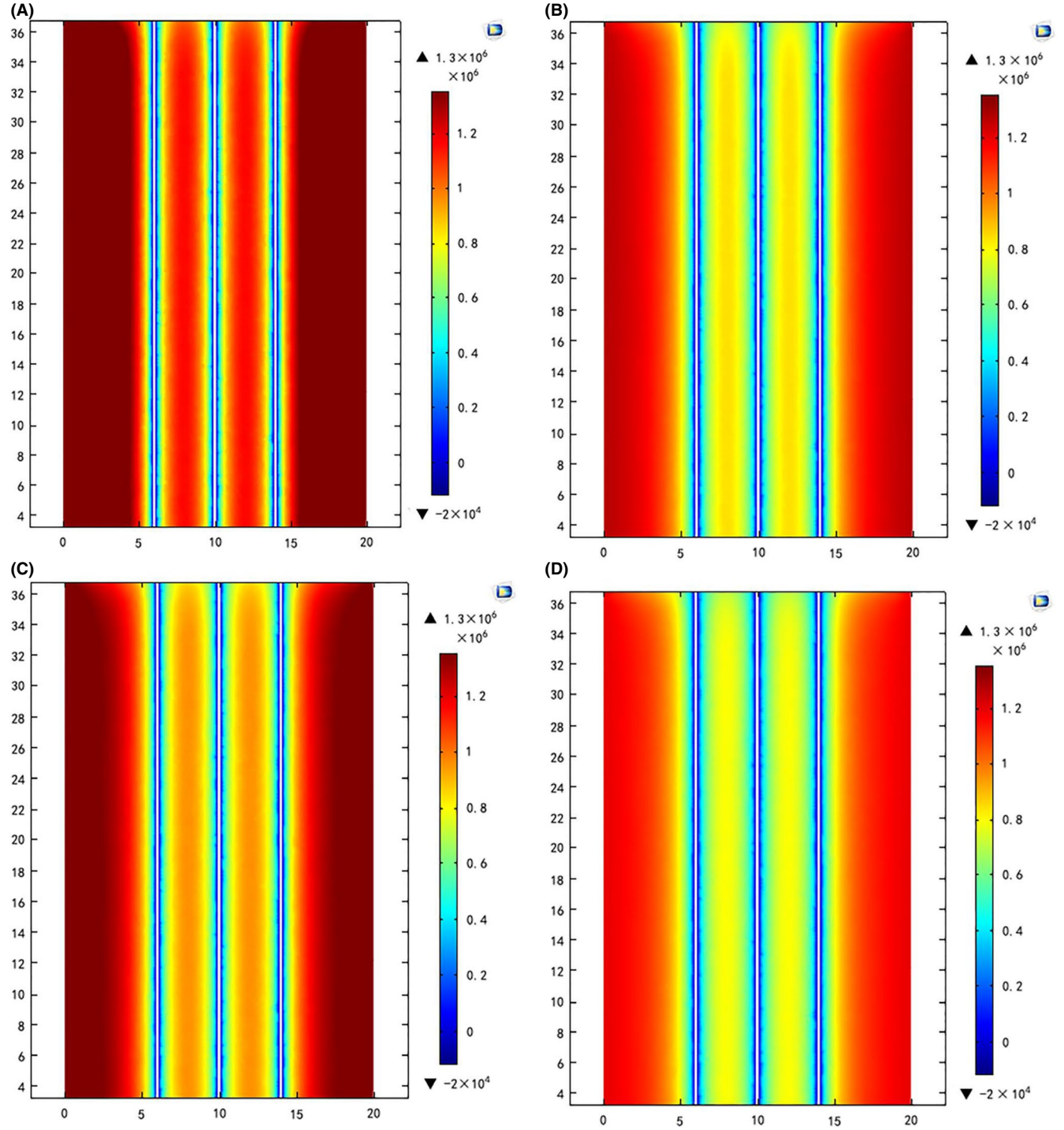

FIGURE 13 Nephogram of gas pressure on a section under different extraction times

gas pressures around the boreholes at these four times were 1.19, 0.92, 0.71, and 0.59 MPa, respectively. The maximum gas pressure around the boreholes was reduced to less than 0.74 MPa at 180 days; therefore, the optimal pre-extraction time was deemed to have been 180 days.

5 | FIELD TEST RESULTS

According to the analysis on the result obtained through numerical simulation, it can be found that the optimal borehole spacing, hole-sealing depth, and pre-extraction time during gas extraction were 3.2~4.2 m, 12 m, and 180 days,

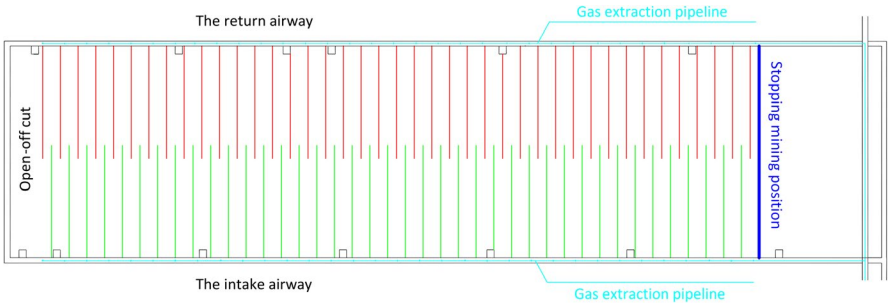

FIGURE 14 Distribution of boreholes for gas extraction

respectively. The research result provides guidance to those concerned with the extraction of gas in mines. By taking mine area as a case study, parameters for gas extraction determined during the aforementioned simulation analysis were applied to the process of gas extraction. Additionally, the parameters for gas extraction were tested to evaluate the effect of gas extraction in practice. Eventually, the parameters for gas extraction were adjusted according to gas extraction data obtained through field testing.

5.1 | Scheme design for gas extraction operations

In the working face for test, the gas in the coal seam was pre-extracted by distributing parallel boreholes along the coal seam (Figure 14). Based on simulation analysis, the optimal borehole spacing, hole-sealing depth, and pre-extraction time were 3.2~4.2 m, 12 m, and 180 days, respectively. The boreholes for gas pre-extraction were parallel and distributed along the two sides of intake and ventilation drifts of the test working face, and the parameters of the boreholes are listed in Table 4.

TABLE 4 Design parameters of boreholes

Parameters	Value	Unit
Diameter of boreholes	90	mm
Included angle between the boreholes and coal wall	90	°
Length of boreholes	85	m
Distance of the boreholes to the floor	0.8	m
Borehole spacing	4.0	m
Hole-sealing depth	12	m
Negative pressure during extraction	20	kPa
Pre-extraction time	180	d

5.2 | Test on the effect of gas extraction

5.2.1 | The amount of extracted gas

Various parameters (including amount of extracted gas, mixed gas flow, and concentration of gas extracted) in the test working face from February to July were calculated: Key statistical results are summarized in Table 5.

According to the data obtained through field test, the amount of extracted gas at the 180th day of gas extraction in the working face is shown in Figure 15. It can be seen that the amount of extracted gas generally rose in an initially unsTABLE manner, then reached the peak, unsteadily decreased, and then stabilized over time: In the early stage, the amount of extracted gas was low (only 2 m^3/min) and fluctuated albeit to an insignificant extent. Over time, with continued gas extraction, the amount of extracted gas increased and fluctuated significantly. At the 100th day of gas extraction, the amount of extracted gas reached its peak (32.21 m^3/min). Thereafter, it fell unsteadily. After gas extraction for 140 days, the amount of extracted gas steadily decreased and then reached a minimum (2 m^3/min) at 180 days. According to the calculated result in Table 5, it can be seen that the total amount of gas extracted from the test working face within six months was 6.8455×10^6 m^3. It is known that the reserves of gas in the working face amounted to 1.75521×10^7 m^3, so the extraction rate of gas from boreholes along the coal seam was 39%, which was satisfactory.

5.2.2 | Reaching the required standard of gas extraction

The gas content in coal seams is measured in field according to *The Direct Method of Determining Coalbed Gas Content in Mines* (GB/T23250). By utilizing the aforementioned method, the gas content in the No. 5 working face was measured (Table 6). After pre-extracting gas from the coal seam at the working face, the gas concentration in the upper corner of the working face during mining stabilized between 0.10% and 0.50% while that in the ventilation drift ranged from 0.0% to 0.20%. Some potential hazards (such as gas concentration exceeding the limit at the upper corner and ventilation drift) were not found in the working face.

According to the index for the content of desorbed gas stipulated in the Article 27 in *Provisions for Gas Drainage Standards in a Coalmine*, the effect of gas extraction in the working face is evaluated. The daily yield of gas from the test working face is set

TABLE 5 Statistics related to amounts of extracted gas in the test working face

Date	Negative pressure during extraction (kPa)	Concentration of gas extracted (%)	Mixed gas flow (m^3/min)	Amount of extracted gas (m^3/min)	Accumulated amount of extracted gas within a month (10^4 m^3)
February	21.2	28.92	116.23	23.97	92.57
March	21.9	33.21	108.12	25.95	114.53
April	22.6	42.16	96.22	26.17	108.36
May	21.5	40.56	98.59	30.13	136.28
June	23.6	29.34	111.66	26.06	114.32
July	22.1	24.07	115.53	24.65	118.49

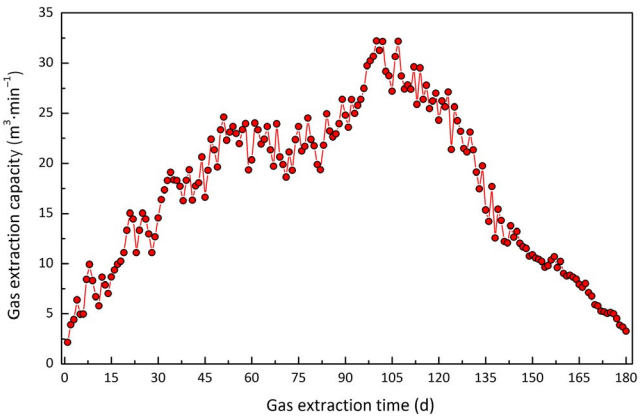

FIGURE 15 Changes in extracted gas flow

as 2.600 t, and the maximum amount of desorbed gas is 3.5494 m^3/t, which is <6 m^3/t. The index for the amount of desorbed gas in coal after gas extraction satisfies the requirement.

5.2.3 | Economic benefit of parameter optimization

During gas extraction from boreholes along the coal seam in the adjacent working face, the gas pre-extraction time, hole-sealing depth, and borehole spacing were designed to be 210 days, 8 m, and 3 m, respectively. Through optimization and adjustment, the gas pre-extraction time was reduced to 180 days while the borehole spacing and hole-sealing depth were 4 and 12 m, respectively. After optimization, the number of boreholes was reduced by 25% and the gas pre-extraction time decreased by 30 d, which not only guaranteed safe production but also decreased the workload associated with gas extraction.

6 | CONCLUSIONS

The following conclusions were drawn.

1. By analyzing the simulated gas extraction data from a single borehole, it can be seen that the longer the gas extraction time, the more significant the reduction in gas pressure in a coal seam, and the more extensive the influence of the boreholes on the gas pressure. In the initial stage of gas extraction, the gas pressure in the coal seams decreased rapidly. Through simulation, the effective radius and radius of influence of boreholes at different extraction times were found and the relationship between the effective radius and extraction time was deduced.

TABLE 6 Gas contents after gas extraction from the coal seam

Distance of the sampling spot to the open-off cut (m)	Loss of gas content (m^3/t)	Amount of desorbed gas content (m^3/t)	Amount of residual gas content(m^3/t)
72	0.8298	3.2299	2.0719
186	0.8383	3.5124	2.1113
293	0.7522	3.2138	2.1867
421	0.9011	2.9438	1.9522
597	0.8876	3.1494	1.9054
730	0.8976	3.2111	2.0479
985	0.7008	3.2729	2.3583
1134	0.8021	3.2751	1.9081
1327	0.8711	3.5109	2.1831
1605	0.9276	3.0326	1.8657

2. By analyzing simulation gas extraction data when using multiple boreholes, it can be found that, due to the superposition effect of boreholes, the reduction in gas pressure around boreholes when conducting gas extraction from multiple boreholes was greater than that from a single borehole. By analyzing changes in gas pressure at different borehole spacings, it can be inferred that the borehole spacing during gas extraction in coal seams from multiple boreholes should be more than twice that of the effective radius of gas extraction. Moreover, the relationship of the optimal borehole spacing with the effective radius and radius of influence of gas extraction was $2r \le L \le r + 0.35R$. Thus, it can be found that the optimal borehole spacing was between 3.2 m and 4.2 m after 180 days of gas extraction.
3. According to the stress-strain mathematical model of the broken zone of coal in the vicinity of a roadway, numerical simulation analysis was carried out to assess the distribution of stress on the coal around the roadway. In this way, the optimal hole-sealing depth was found to be 12 m. Based on a fluid-solid coupling mathematical model, a solid model was established to simulate the process of gas extraction under different extraction times at a borehole spacing of 4 m. The optimal pre-extraction time was found to be 180 days according to the simulated results.
4. Based on the result obtained through numerical simulation, parameters for gas extraction related to the working face under test were optimized. The result acquired through field testing showed that the effect of gas extraction after optimizing the parameters for gas extraction reached the required standard. And, it was found that the number of boreholes in the test working face decreased by 25% and the gas pre-extraction time was reduced by 30 d. This not only guaranteed safe production, but also reduced the workload associated with such gas extraction.

CONFLICT OF INTEREST

The authors declare no conflict of interest.

ORCID

Pan Wei https://orcid.org/0000-0002-1770-3787
Shoujian Peng https://orcid.org/0000-0002-1801-4246

REFERENCES

1. Wei P, Liang Y, Zhao S, Peng S, Li X, Meng R. Characterization of pores and fractures in soft coal from the no. 5 Soft coalbed in the Chenghe mining area. *Processes*. 2019;7(1):13.
2. Qianting HU, Yunpei L, Han W, Quanle Z, Haitao S. Intelligent and integrated techniques for coalbed methane (CBM) recovery and reduction of greenhouse gas emission. *Environ Sci Pollut Res*. 2017;24(21):17651-17668.
3. Karacan CÖ, Ruiz FA, Cotè M, Phipps S. Coal mine methane: a review of capture and utilization practices with benefits to mining safety and to greenhouse gas reduction. *Int J Coal Geol*. 2011;86(2–3):121-156.
4. Lau HC, Li H, Huang S. Challenges and opportunities of coalbed methane development in China. *Energy Fuels*. 2017;31(5):4588-4602.
5. Zhou F, Xia T, Wang X, Zhang Y, Sun Y, Liu J. Recent developments in coal mine methane extraction and utilization in China: a review. *J Nat Gas Sci Eng*. 2016;31:437-458.
6. Li X, Li Z, Wang E, et al. Pattern recognition of mine microseismic and blasting events based on wave fractal features. *Fractals*. 2018;26(03):1850029.
7. Wang G, Wu M, Wang R, Xu H, Song X. Height of the mining-induced fractured zone above a coal face. *Eng Geol*. 2017;216:140-152.
8. Li Q, Lin B, Yang W, Zhai C, Hao Z. Gas control technology and engineering practice for three-soft coal seam with low permeability in XuanGang region, China. *Proc Eng*. 2011;26:560-569.
9. Guo H, Todhunter C, Qu Q, Qin Z. Longwall horizontal gas drainage through goaf pressure control. *Int J Coal Geol*. 2015;150:276-286.
10. Lin H, Huang M, Li S, Zhang C, Cheng L. Numerical simulation of influence of Langmuir adsorption constant on gas drainage radius of drilling in coal seam. *Int J Min Sci Technol*. 2016;26(3):377-382.
11. Cheng YP, Fu JH, Yu QX. Development of gas extraction technology in coal mines of China. *J Min Saf Eng*. 2009;2:127-139.
12. Yin GZ, Li MH, Li SZ, et al. 3D numerical simulation of gas drainage from boreholes based on solid gas coupling model of coal containing gas. *J China Coal Soc*. 2013;38(4):535-541.
13. Xu MG, Wei P, Li SG, et al. Experimental study on overburden migration and fracture evolution law of "three soft" coal seam fully mechanized working-face. *J China Coal Soc*. 2017;42(S1):122-127.
14. Xia B, Zhao B, Lu Y, Liu C, Song C. Drainage radius after high pressure water jet slotting based on methane flow field. *Int J Heat Technol*. 2016;34(3):507-512.
15. Hu S, Zhou F, Liu Y, Xia T. Effective stress and permeability redistributions induced by successive roadway and borehole excavations. *Rock Mech Rock Eng*. 2015;48(1):319-332.
16. Langmuir I. The constitution and fundamental properties of solids and liquids. Part I. Solids. *J Am Chem Soc*. 1916;38(11):2221-2295.
17. Langmuir I. The constitution and fundamental properties of solids and liquids II. Liquids. *J Am Chem Soc*. 1917;39(9):1848-1906.
18. Ettinger I, Eremin I, Zimakov B, et al. Natural factors influencing coal sorption properties. I. Petrography and sorption properties of coals. *Fuel*. 1966;45(4):267.
19. Dubinin MM. The potential theory of adsorption of gases and vapors for adsorbents with energetically nonuniform surfaces. *Chem Rev*. 1960;60(2):235-241.
20. Wohleber DA, Manes M. Application of the Polanyi adsorption potential theory to adsorption from solution on activated carbon. III. Adsorption of miscible organic liquids from water solution. *J Phys Chem*. 1971;75(24):3720-3723.
21. Manes M, Hofer L. Application of the Polanyi adsorption potential theory to adsorption from solution on activated carbon. *J Phys Chem*. 1969;73(3):584-590.
22. Wood GO. Affinity coefficients of the Polanyi/Dubinin adsorption isotherm equations: a review with compilations and correlations. *Carbon*. 2001;39(3):343-356.

23. Chen XJ. Modeling of experimental adsorption isotherm data. *Information*. 2015;6(1):14-22.
24. Foo KY, Hameed BH. Insights into the modeling of adsorption isotherm systems. *Chem Eng J*. 2010;156(1):2-10.
25. Dubinin MM. Generalization of the theory of volume filling of micropores to nonhomogeneous microporous structures. *Carbon*. 1985;23(4):373-380.
26. Hutson ND, Yang RT. Theoretical basis for the Dubinin-Radushkevitch (DR) adsorption isotherm equation. *Adsorption*. 1997;3(3):189-195.
27. Skopp J. Derivation of the Freundlich adsorption isotherm from kinetics. *J Chem Educ*. 2009;86(11):1341.
28. Wang Y, Dusseault MB. Borehole yield and hydraulic fracture initiation in poorly consolidated rock strata—Part I. Impermeable media[C]//International journal of rock mechanics and mining sciences & geomechanics abstracts. *Pergamon*. 1991;28(4):235-246.
29. Wang Y, Dusseault MB. Borehole yield and hydraulic fracture initiation in poorly consolidated rock strata—Part II. Permeable media[C]//International journal of rock mechanics and mining sciences & geomechanics abstracts. *Pergamon*. 1991;28(4):247-260.
30. Seidle JR, Huitt LG.Experimental measurement of coal matrix shrinkage due to gas desorption and implications for cleat permeability increases International meeting on petroleum Engineering. Society of Petroleum Engineers, Paper SPE 30010, 1995, Beijing, China (14–17 November).
31. Peng Y, Liu J, Wei M, Pan Z, Connell LD. Why coal permeability changes under free swellings: new insights. *Int J Coal Geol*. 2014;133:35-46.
32. Wu YU, Liu J, Elsworth D, Siriwardane H, Miao X. Evolution of coal permeability: contribution of heterogeneous swelling processes. *Int J Coal Geol*. 2011;88(2-3):152-162.
33. Zhang HB, Liu JS, Elsworth D. How sorption-induced matrix deformation affects gas flow in coal seams: a new FE model. *Int J Rock Mech Min Sci*. 2008;45(8):1226-1236.
34. Connell LD. Coupled flow and geomechanical processes during gas production from coal seams. *Int J Coal Geol*. 2009;79(1-2):18-28.
35. Shi JQ, Durucan S. Drawdown induced changes in permeability of coalbeds: a new interpretation of the reservoir response to primary recovery. *Transp Porous Media*. 2004;56(1):1-16.
36. Shi JQ, Durucan S. A model for changes in coalbed permeability during primary and enhanced methane recovery. *SPE Reserv Eval Eng*. 2005;8(04):291-299.
37. Zheng C, Kizil M, Chen Z, Aminossadati S. Effects of coal damage on permeability and gas drainage performance. *Int J Min Sci Technol*. 2017;27(5):783-786.
38. Zeng QS, Wang ZM. A new cleat volume compressibility determination method and corresponding modification to coal permeability model. *Transp Porous Media*. 2017;119(3):689-706.
39. Robertson EP, Christiansen RL. Modeling permeability in coal using sorption-induced strain data[R]. Idaho National Laboratory (INL).2005.
40. Robertson EP, Christiansen RL. A permeability model for coal and other fractured, sorptive-elastic media[R]. Idaho National Laboratory (INL).2006.
41. Guo P, Cheng Y, Jin K, Li W, Tu Q, Liu H. Impact of effective stress and matrix deformation on the coal fracture permeability. *Transp Porous Media*. 2014;103(1):99-115.
42. Xie J, Gao M, Yu B, Zhang RU, Jin W. Coal permeability model on the effect of gas extraction within effective influence zone. *Geomech Geophys Geo-Energy Geo-Resour*. 2015;1(1–2):15-27.
43. Hu G-Z, Wang H-T, Tan H-X, Fan X-G, Yuan Z-G. Gas seepage equation of deep mined coal seams and its application. *J China Univ Min Technol*. 2008;18(4):483-487.
44. Whitaker S. Flow in porous media I: a theoretical derivation of Darcy's law. *Transp Porous Media*. 1986;1(1):3-25.
45. Gao F, Xue YI, Gao Y, Zhang Z, Teng T, Liang X. Fully coupled thermo-hydro-mechanical model for extraction of coal seam gas with slotted boreholes. *J Nat Gas Sci Eng*. 2016;31:226-235.
46. Whittles DN, Lowndes IS, Kingman SW, Yates C, Jobling S. The stability of methane capture boreholes around a long wall coal panel. *Int J Coal Geol*. 2007;71(2-3):313-328.
47. Yang TH, Xu T, Liu HY, Tang CA, Shi BM, Yu QX. Stress–damage–flow coupling model and its application to pressure relief coal bed methane in deep coal seam. *Int J Coal Geol*. 2011;86(4):357-366.
48. Peng R, Ju Y, Wang JG, Xie H, Gao F, Mao L. Energy dissipation and release during coal failure under conventional triaxial compression. *Rock Mech Rock Eng*. 2015;48(2):509-526.
49. Xu P, Yu B. Developing a new form of permeability and Kozeny-Carman constant for homogeneous porous media by means of fractal geometry. *Adv Water Resour*. 2008;31(1):74-81.

How to cite this article: Wei P, Huang C, Li X, Peng S, Lu Y. Numerical simulation of boreholes for gas extraction and effective range of gas extraction in soft coal seams. *Energy Sci Eng*. 2019;7:1632–1648. https://doi.org/10.1002/ese3.377